Surface Tension and Interfacial Tension of Binary Organic Liquid Mixtures

Heike Kahl, Tino Wadewitz, and Jochen Winkelmann*

Institute of Physical Chemistry, Martin-Luther University Halle-Wittenberg, D-06217 Merseburg, Germany

The pendant drop method, combined with efficient temperature control of the measuring cell, allows high precision measurements of both surface tension and interfacial tension. The surface tensions and liquid densities of mixtures of cyclohexane + heptane, cyclohexane + propanone, and toluene + propanone have been determined at a normal pressure of 1 bar over the temperature range from 287 K to 317 K. The surface tension data could be parametrized with a cubic polynomial. Gibbs excess surface concentrations are derived from our experimental data, and the influence of activity coefficients is discussed. The high precision pendant drop apparatus allows accurate measurements of the interfacial tension in systems with liquid−liquid phase separation. In binary mixtures of heptane + *N*,*N*-dimethylformamide, heptane + *N*-methyl-2-pyrrolidone, and decane + *N*,*N*-dimethylformamide, the interfacial tension was measured over a wide temperature range close to the critical solution point. The densities of the corresponding liquid phases were obtained by buoyancy measurements. The accuracy of the density measurements is $\Delta\rho = \pm 0.0001$ g·cm^{-3} for the vibrating tube densimeter; for the buoyancy measurements we find $\Delta\rho = \pm 0.0005$ g·cm^{-3}. The reproducibility of the surface tension measurements is generally better than $\Delta\sigma = \pm 0.50\%$ at the 95% confidence level. Standard deviations for all experimental values are given in the tables. The resulting data are parametrized using polynomial and Wegener expansion type equations.

Introduction

The precise measurement of surface and interfacial tensions is of outstanding importance in many scientific and technological areas. As commonly accepted, we define as surface tension all tensions measured in systems with free surfaces, that is, for liquid phases (pure liquids and liquid mixtures) in contact with a gas or vapor. The term interfacial tension is used for interfaces where two immiscible liquid phases are in contact. As a fundamental parameter, surface tension is the single most accessible experimental parameter that describes the thermodynamic state and contains at least implicit information on the internal structure of a liquid interface. Apart from this theoretical interest, a detailed understanding of the behavior of a vapor−liquid interface, such as enrichment of one component in a liquid surface, is important for modeling a distillation process. On the other hand, liquid−liquid interfaces have far-reaching practical consequences in very wide areas of application. The selection of suitable solvents for a liquid−liquid extraction in petrochemical processing depends to a large extent on both liquid−liquid solubility and interfacial tension. Surface tensions have been measured for a long time, and collections of experimental data for pure liquids and some binary liquid mixtures exist.[1−3] A critical review reveals that systematic investigations of liquid−liquid interfaces are rather rare, especially in a wide temperature and concentration range. High quality experimental data of surface and interfacial tensions form the basis for a successful modeling and for theoretical calculations of interfacial properties.[4−8] Therefore, further precision measurements are badly needed. Because of its high flexibility and precision, the pendant drop method is the favored experimental technique to investigate both interfacial and surface tensions over several orders of magnitude, ranging from 0.01 mN/m for interfacial tensions close to the critical solution point up to 80 mN/m in the case of water. In this respect it is superior to most other commonly used experimental methods such as the Wilhelmy plate or spinning drop methods.[9−12] The amount of the sample is small, and it is possible to measure both surface and interfacial tensions with high accuracy even under high pressure.[13−15] Extremely small interfacial tensions in the vicinity of the critical solution points[16,17] can be determined where spinning drop measurements usually fail because of their low temperature stability.

* To whom correspondence should be addressed. E-mail: winkelmann@chemie.uni-halle.de.

Experimental Section

Reagents. Cyclohexane pa. with a purity of >99.5% (by GC) and a water content of 0.01% was supplied by Fa. Riedel-de Haen; *N*,*N*-dimethylformamide pa. with a purity of >99.5% (by GC) and a water content of 0.15% was supplied by Fa. Fluka; and heptane pa. with a purity of >99.0% (by GC) and a water content of 0.01%, decane pa. with a purity of >99.5% (by GC) and a water content of 0.01%, propanone pa. with a purity of >99.5% (by GC) and a water content of 0.2%, toluene pa. with a purity of >99.5% (by GC) and a water content of 0.03%, and *N*-methyl-2-pyrrolidone pa. with a purity of >99.5% (by GC) and a water content of 0.1% were supplied by Fa. Merck, Darmstadt, Germany. All substances were dried over molecular sieves ZEOSORB A4/A3 and stored in a dark place.

Measuring Procedure and Calibration. (a) Surface and Interfacial Tension. The experimental setup[18] to determine both surface and interfacial tension is shown in Figure 1a.

10.1021/je034062r CCC: $25.00
Published on Web 10/29/2003

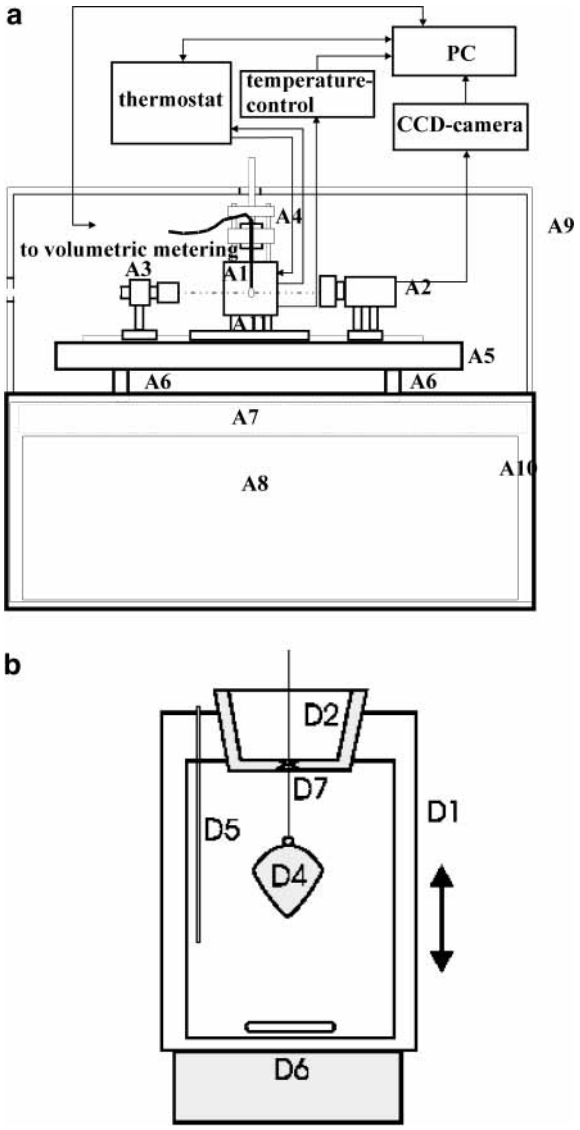

Figure 1. (a) Pendant drop apparatus: A1, measuring cell; A2, CCD camera; A3, light source coupling; A4, capillary; A5, vibration-damped breadboard; A6, vibration-control system; A7, slab; A8, sand bed; A9, dust jacket; A10, brick base; A11, *xyz*-positioning table. (b) Equipment for buoyancy measurements: D1, movable barrel; D2, Teflon stopper; D3, scale; D4, glass vessel filled with lead; D5, thermistor; D6, stirrer; D7, electrical contact.

It is discussed in detail in a previous paper.[19] The drop, formed at the end of the capillary, is illuminated by glass fiber optics aligned parallel by a light source coupling. The pendant drop profiles are extracted from the drop images and analyzed by means of the ADSA-software,[10,20] which ensures a high quality contour extraction and a very precise interfacial tension calculation by numerical solution of the Laplace equation. For each sample we develop four different drops and record 10 images of each drop.

To measure the interfacial tensions of samples with phase separation, mixtures were directly prepared in the measuring cell and equilibrated. When the temperature control shows that, usually after 1 h or more, the thermal equilibrium is reached, the sample is stirred once again and both phases are allowed to separate. The phase separation could be followed up using the CCD camera of the pendant drop system. Then drops of the lower phase are developed in the upper phase and the images are recorded. We record 10 images of each drop. The relative uncertainty, which depends on temperature and concentration, is given for each data point.

Table 1. Comparison of the Measured Liquid Density, ρ, of Heptane with Values from the Literature[21]

T/K	ρ/g·cm^{-3}(this work)	ρ/g·cm^{-3}(Vargaftik[21])
293.15	0.6838	0.6838
303.15	0.6752	0.6751
313.15	0.6665	0.6665
323.15	0.6577	0.6579
333.15	0.6487	0.6491

(b) Density. The densities of homogeneous liquid mixtures, needed for the numerical solution of the Laplace equation, are determined using a vibrating tube densimeter (DMA 60 Fa. Anton Paar) with temperature control of ±0.01 K. At first, the densimeter was calibrated with dry air and water to measure the densities of pure heptane. A comparison of these experimental densities with data from the literaure[21] is shown in Table 1.

To measure the densities of the other substances and those of the binary mixtures for the calibration of the densimeter at each temperature, twice distilled water and pure heptane were used. The density range between heptane and water is smaller than that between air and water, so that the resulting densities are more precise. The accuracy of the measured densities is considered to be $\Delta\rho = \pm 0.0001$ g·cm^{-3}.

The measurement of density differences between both phases in liquid−liquid equilibrium is a much more complicated task, especially when approaching the vicinity of the critical solution temperature. The use of a vibration tube densimeter would require that samples of both liquid phases have to be measured separately. In this process we faced serious problems with demixing and change in composition as well as temperature stability. For that reason, buoyancy measurements were used to determine the density differences between the liquid phases. The experimental setup[18] is given in Figure 1b.

The samples are placed inside of a temperature controlled movable barrel, closed with a Teflon stopper. To control the temperature, a JULABO FP 40 MH thermostat together with a thermistor is used, which enables us to keep the temperature constant to $\Delta T = \pm 0.005$ K over the measuring period. A precision microbalance is placed above the barrel, which allows mass determination accurate to ±0.00001 g. A nickel wire linked the balance with a glass vessel filled with lead. Contrary to the case of Chaar et al.,[22] it has the shape of an inverse drop, so that minimal liquid will adhere. An electrical contact inside the stopper ensured that the load is hanging free. The mass m_T of the plumb filled glass vessel was determined at several temperatures, and the cubic expansion coefficient of the used glass vessel was taken into account. This yields

$$m_T = A + B[\rho_T(1 + 3\alpha\Delta T)], \quad \Delta T = T - T_{ref}. \qquad (1)$$

where $T_{ref} = 298.24$ K denotes the reference temperature and α is the thermal expansion coefficient. Parameters A and B are calculated using calibration measurements of several values of pure substances (heptane, toluene, cyclohexane, and air). To calibrate the equipment, we measured 174 reference points.

The sample was filled in the barrel and brought to constant temperature. Then the mixture was stirred once again, and after phase equilibration the mass of the load was determined in each phase: at first in the upper and afterward in the lower phase. This procedure was repeated

Table 2. Experimental Surface Tension, σ, from 287.81 K to 327.88 K for Cyclohexane (1) + Heptane (2) Measured with the Pendant Drop Apparatus, and the Mixing Parameters, σ_{112} and σ_{122}, Obtained from Eq 2

	σ/mN·m^{-1}				
x_1	T/K = 287.81	T/K = 297.82	T/K = 307.86	T/K = 317.86	T/K = 327.88
1.0000	25.34 ± 0.04	24.20 ± 0.03	23.02 ± 0.03	21.84 ± 0.04	20.71 ± 0.03
0.8980	24.39 ± 0.08	23.32 ± 0.07	22.18 ± 0.07	21.07 ± 0.05	19.98 ± 0.05
0.8054	23.84 ± 0.01	22.72 ± 0.06	21.64 ± 0.05	20.56 ± 0.05	19.48 ± 0.05
0.7003	23.08 ± 0.03	22.14 ± 0.06	21.06 ± 0.06	20.01 ± 0.06	18.95 ± 0.05
0.6002	22.62 ± 0.01	21.57 ± 0.06	20.53 ± 0.10	19.55 ± 0.06	18.44 ± 0.12
0.4984	22.27 ± 0.01	21.21 ± 0.02	20.19 ± 0.03	19.16 ± 0.07	17.99 ± 0.08
0.4010	21.88 ± 0.01	20.90 ± 0.02	19.87 ± 0.01	18.82 ± 0.06	17.52 ± 0.10
0.3078	21.65 ± 0.01	20.52 ± 0.01	19.58 ± 0.01	18.53 ± 0.01	17.41 ± 0.21
0.2022	21.31 ± 0.01	20.25 ± 0.02	19.25 ± 0.01	18.36 ± 0.01	17.05 ± 0.10
0.1022	20.91 ± 0.01	19.95 ± 0.03	18.91 ± 0.01	17.91 ± 0.04	16.83 ± 0.05
0.0000	20.70 ± 0.02	19.63 ± 0.05	18.68 ± 0.03	17.76 ± 0.05	16.68 ± 0.03
σ_{112}	66.41 ± 0.27	63.63 ± 0.15	60.64 ± 0.17	57.86 ± 0.28	55.20 ± 0.27
σ_{122}	65.40 ± 0.27	62.19 ± 0.15	59.10 ± 0.17	55.81 ± 0.26	51.37 ± 0.27

Table 3. Experimental Liquid Densities, ρ, from 283.15 K to 333.15 K for Cyclohexane (1) + Heptane (2)

	ρ/g·cm^{-3} at the following values of T/K										
x_1	283.15	288.15	293.15	298.15	303.15	308.15	313.15	318.15	323.15	328.15	333.15
1.0000	0.7879	0.7832	0.7786	0.7739	0.7692	0.7644	0.7596	0.7548	0.7500	0.7452	0.7403
0.8980	0.7742	0.7697	0.7651	0.7605	0.7558	0.7512	0.7465	0.7418	0.7371	0.7323	0.7275
0.8054	0.7615	0.7580	0.7535	0.7490	0.7444	0.7398	0.7352	0.7306	0.7259	0.7212	0.7165
0.7003	0.7508	0.7464	0.7420	0.7375	0.7330	0.7284	0.7239	0.7193	0.7147	0.7100	0.7053
0.6002			0.7288	0.7256	0.7220	0.7181	0.7138	0.7093	0.7047	0.7001	0.6955
0.4984	0.7308	0.7265	0.7222	0.7178	0.7133	0.7089	0.7044	0.6999	0.6954	0.691	0.6862
0.4010	0.7223	0.7179	0.7136	0.7092	0.7048	0.7004	0.6960	0.6915	0.6869	0.6824	0.6778
0.3078	0.7146	0.7104	0.7061	0.7017	0.6974	0.6930	0.6886	0.6841	0.6796	0.6751	0.6705
0.2022	0.7065	0.7022	0.6980	0.6936	0.6893	0.6850	0.6806	0.6761	0.6717	0.6672	
0.1022	0.6992	0.6950	0.6908	0.6865	0.6822	0.6778	0.6735	0.6690	0.6646	0.6601	0.6555
0.0000	0.6922	0.6880	0.6838	0.6795	0.6752	0.6709	0.6665	0.6621	0.6577	0.6532	0.6487

Table 4. Experimental Surface Tension, σ, from 287.81 K to 327.88 K for Mixtures of Toluene (1) + Propanone (2) Measured with the Pendant Drop Apparatus, and the Mixing Parameters Obtained from Eq 2

	σ/mN·m^{-1}				
x_1	T/K = 287.81	T/K = 297.82	T/K = 307.86	T/K = 317.86	T/K = 327.88
0.0000	23.94 ± 0.06	22.78 ± 0.01	21.59 ± 0.01	20.33 ± 0.01	19.01 ± 0.03
0.1000	24.56 ± 0.04	23.28 ± 0.04	22.08 ± 0.02	20.90 ± 0.02	19.74 ± 0.07
0.2002	25.24 ± 0.05	23.78 ± 0.03	22.58 ± 0.03	21.44 ± 0.02	20.32 ± 0.06
0.3002	25.89 ± 0.01	24.36 ± 0.04	23.10 ± 0.03	22.18 ± 0.04	21.07 ± 0.08
0.3997	26.46 ± 0.02	24.93 ± 0.03	23.77 ± 0.04	22.67 ± 0.04	21.80 ± 0.08
0.4973	27.10 ± 0.04	25.55 ± 0.04	24.40 ± 0.03	23.25 ± 0.03	22.20 ± 0.06
0.6011	27.68 ± 0.05	26.00 ± 0.04	25.00 ± 0.03	24.11 ± 0.03	22.97 ± 0.08
0.7004	28.24 ± 0.05	26.50 ± 0.01	25.40 ± 0.07	24.40 ± 0.05	23.56 ± 0.01
0.7998	28.48 ± 0.02	27.10 ± 0.14	26.00 ± 0.02	24.99 ± 0.02	23.83 ± 0.03
0.8982	28.73 ± 0.01	27.33 ± 0.09	26.24 ± 0.03	25.20 ± 0.05	24.14 ± 0.04
1.0000	28.93 ± 0.03	27.76 ± 0.05	26.60 ± 0.05	25.46 ± 0.04	24.29 ± 0.04
σ_{112}	86.16 ± 0.22	80.30 ± 0.26	77.66 ± 0.26	75.11 ± 0.39	72.23 ± 0.40
σ_{122}	77.93 ± 0.22	73.08 ± 0.26	69.01 ± 0.26	66.01 ± 0.39	63.42 ± 0.39

at each temperature. The accuracy of the measured densities in both liquid phases is considered to be $\Delta\rho = \pm 0.0005$ g·cm^{-3}.

Results and Discussion

Surface Tension. In this section the results of surface tension measurements, using a pendant drop apparatus and corresponding liquid densities obtained with a vibration tube densimeter, are presented. Three homogeneous binary systems were investigated. At several temperatures mixtures of cyclohexane + heptane and + propanone as well as mixtures of propanone + toluene were studied over the whole concentration range. The isothermal experimental data are parametrized using the following cubic polynomial in the mole fractions of both components, which can easily be extended to describe results in ternary mixtures, too:

$$\sigma = \sigma_1^{0} x_1^{3} + \sigma_{112} x_1^{2} x_2 + \sigma_{122} x_1 x_2^{2} + \sigma_2^{0} x_2^{3} \qquad (2)$$

The parameters σ_i^0 denote the experimental surface tension values of the pure substances, whereas the binary parameters σ_{122} and σ_{122} are fitted to the measured raw data. In this way eq 2 provides a simple tool for isothermal interpolation of surface tensions in these mixtures with an accuracy that is within the experimental uncertainty. The experimental data for these three systems are given in the following tables: Tables 2, 4, and 6 contain the surface tension data and their respective standard deviations of the three systems together with the binary parameters of eq 2 at each temperature. The corresponding tables (Tables 3, 5, and 7) present the liquid densities of these systems used for the evaluation of surface tension.

Figure 2a shows the results of the experimental surface tension measurements in the nonpolar system cyclohexane (1) + heptane (2) in comparison with experimental data obtained by Herrmann[23] using a ring method. The solid lines represent the parametrization according to eq 2; they are in very good agreement with the experiment. Even the

Table 5. Experimental Liquid Densities, ρ, from 283.15 K to 333.15 K for Mixtures of Toluene (1) + Propanone (2)

	ρ/g·cm^{-3} at the following values of T/K										
x_1	283.15	288.15	293.15	298.15	303.15	308.15	313.15	318.15	323.15	328.15	333.15
0.0000	0.8032	0.7982	0.7926	0.7870	0.7812	0.7754	0.7696	0.7625	0.7562	0.7493	0.7423
0.1000	0.8151	0.8098	0.8042	0.7988	0.7933	0.7877	0.7820	0.7762	0.7702	0.7640	0.7573
0.2002	0.8235	0.8182	0.8125	0.8071	0.8016		0.7904	0.7846	0.7789	0.7732	0.7675
0.3002	0.8322	0.8268	0.8214	0.8161	0.8108	0.8055	0.8001	0.7946	0.7891	0.7835	0.7781
0.3997	0.8412	0.8361	0.8307	0.8256	0.8204	0.8151	0.8097	0.8042	0.7986	0.7929	0.7873
0.4973	0.8476	0.8426	0.8373	0.8323	0.8272	0.8221	0.8169	0.8116	0.8063	0.8010	0.7956
0.6011	0.8547	0.8499	0.8446	0.8397	0.8347	0.8297	0.8247	0.8195	0.8144	0.8092	0.8039
0.7004	0.8608	0.8560	0.8509	0.8461	0.8413	0.8364	0.8314	0.8264		0.8163	0.8112
0.7998	0.8664	0.8617	0.8566	0.8519	0.8472	0.8424	0.8376	0.8327	0.8277	0.8228	0.8178
0.8982	0.8715	0.8669	0.8619	0.8573	0.8526	0.8479	0.8432	0.8384	0.8336	0.8287	0.8238
1.0000	0.8759	0.8714	0.8669	0.8624	0.8578	0.8532	0.8486	0.8439	0.8392	0.8345	0.8298

Table 6. Experimental Surface Tension, σ, from 287.81 K to 317.86 K for Mixtures of Cyclohexane (1) + Propanone (2) Measured with the Pendant Drop Apparatus, and the Mixing Parameters, σ_{112} and σ_{122}, Obtained Using Eq 2

	σ/m·Nm^{-1}			
x_1	T/K = 287.81	T/K = 297.82	T/K = 307.86	T/K = 317.86 K
0.0000	23.94 ± 0.06	22.78 ± 0.01	21.59 ± 0.01	20.33 ± 0.01
0.1002	23.54 ± 0.02	22.25 ± 0.03	21.03 ± 0.01	19.91 ± 0.01
0.2001	23.19 ± 0.06	22.02 ± 0.03	20.78 ± 0.03	19.63 ± 0.03
0.2993	23.23 ± 0.04	22.02 ± 0.04	20.82 ± 0.02	19.63 ± 0.01
0.3979	23.33 ± 0.02	22.08 ± 0.02	20.89 ± 0.02	19.70 ± 0.04
0.4964	23.58 ± 0.01	22.22 ± 0.02	21.14 ± 0.02	20.00 ± 0.01
0.6000	23.91 ± 0.06	22.53 ± 0.03	21.35 ± 0.03	20.30 ± 0.16
0.6975	24.31 ± 0.10	22.84 ± 0.04	21.60 ± 0.10	20.56 ± 0.04
0.7993	24.69 ± 0.06	23.24 ± 0.03	22.08 ± 0.04	21.04 ± 0.05
0.8994	25.12 ± 0.05	23.82 ± 0.13	22.58 ± 0.05	21.46 ± 0.08
1.0000	25.34 ± 0.04	24.20 ± 0.02	23.02 ± 0.03	21.84 ± 0.04
σ_{112}	73.71 ± 0.18	68.17 ± 0.24	64.66 ± 0.34	61.91 ± 0.18
σ_{122}	65.76 ± 0.18	62.68 ± 0.24	59.08 ± 0.34	55.52 ± 0.18

Table 7. Experimental Liquid Densities, ρ, from 288.15 K to 318.15 K for Mixtures of Cyclohexane (1) + Propanone (2)

	ρ/g·cm^{-3}			
x_1	T/K = 288.15	T/K = 298.15	T/K = 308.15	T/K = 318.15
0.0000	0.7982	0.7870	0.7754	0.7625
0.1002	0.7900	0.7797	0.7684	0.7569
0.2001	0.7866	0.7753	0.7642	0.7530
0.2993	0.7832	0.7723	0.7614	0.7502
0.3979	0.7811	0.7697	0.7596	0.7486
0.4964	0.7797	0.7692	0.7586	0.7478
0.6000	0.7789	0.7686	0.7582	0.7476
0.6975	0.7789	0.7687	0.7599	0.7483
0.7993	0.7794	0.7695	0.7596	0.7496
0.8994	0.7807	0.7711	0.7614	0.7516
1.0000	0.7832	0.7739	0.7644	0.7548

binary parameters show an almost linear temperature dependence, whereas the older data yield binary parameters with a considerable scatter. Mixing parameters, which were obtained from fitting Wilhelmy plate measurements, show a significantly larger scatter (inset in Figure 2a).

The variation of surface tension with the composition of a mixture contains important information on enrichment effects of one component within the interface. The Gibbs adsorption isotherm provides the theoretical background; it relates the Gibbs excess concentration Γ_{21} to the surface tension gradient

$$\Gamma_{21} = -\left(\frac{\partial\sigma}{\partial x_2}\right)_{T,p} \frac{x_2}{RT}\left(1 + \frac{\partial \ln \gamma_2}{\partial \ln x_2}\right)_{T,p}^{-1} \qquad (3)$$

In the limiting case of an ideal mixture, eq 3 simplifies to

$$\Gamma_{21} = -\left(\frac{\partial\sigma}{\partial x_2}\right)_{T,p} \frac{x_2}{RT} \qquad (4)$$

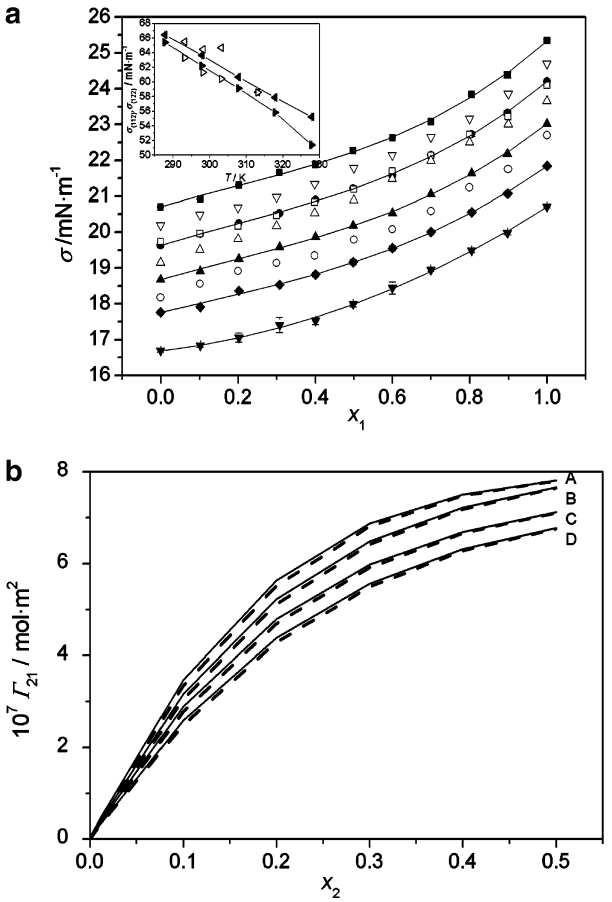

Figure 2. (a) Experimental surface tension, σ, of the binary mixture cyclohexane (1) + heptane (2) measured with the pendant drop apparatus. This work: ■, T = 287.81 K; ●, T = 297.81 K; ▲, T = 307.86 K; ◆, T = 317.86 K; ▼, T = 327.88 K. Herrmann:[23] ▽, T = 293.15 K; □, T = 298.15 K; △, T = 303.15 K; ○, T = 313.15 K. The full lines are the model calculations according to eq 2. Inset: Binary mixing parameter, σ_{112}, obtained from surface tension measurements. Solid triangle pointing left, this work; open triangle pointing left, based on data obtained from Herrmann.[23] Mixing parameter, σ_{122}. Solid triangle pointing right, this work; open triangle pointing right, based on data obtained from Herrmann[23] using eq 2. **(b)** Influence of the activity coefficients on the Gibbs excess concentration, Γ_{21}, of heptane in the system cyclohexane (1) + heptane (2) obtained by surface tension measurements: using eq 3 (full lines, Γ_{real}) and eq 4 (dashed lines, Γ_{ideal}). (A) T = 287.81 K; (B) T = 297.81 K; (C) T = 307.86 K; (D) T = 317.86 K.

which is often applied to systems where the assumption of γ_2 being 1 is not fulfilled. In addition to that, the expression for Γ_{21} is derived under the assumption $\Gamma_1 = 0$, that is, no enrichment of substance 1 in the interface. Therefore, eq 3 should only be applied in the concentration range $0 \le x_2 \le 0.5$, where component 2 is really the solute.

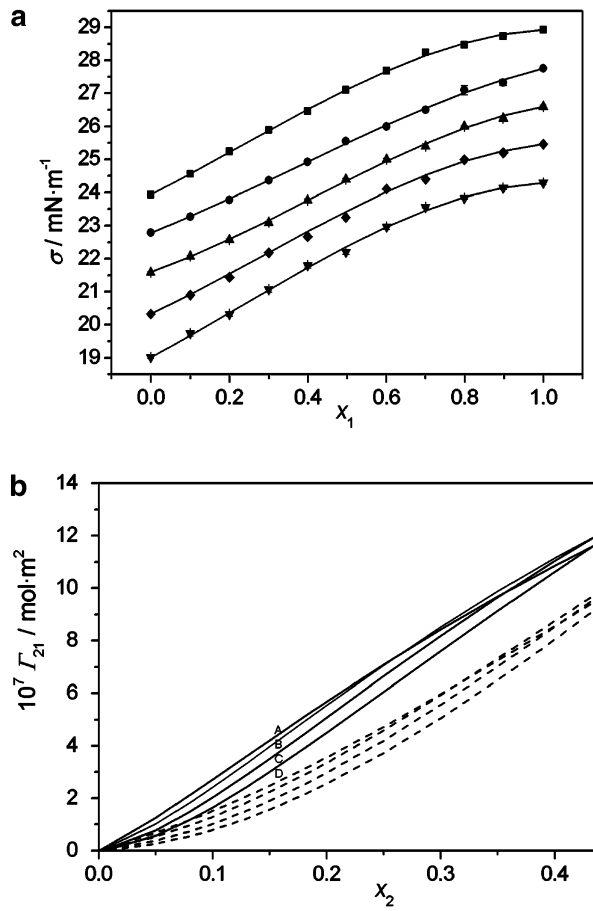

Figure 3. **(a)** Experimental surface tension, σ, of the binary mixtures of toluene (1) + propanone (2) measured with the pendant drop apparatus: ■, T = 287.81 K; ●, T = 297.82 K; ▲, T = 307.86 K; ◆, T = 317.86 K; ▼, T = 327.88 K. The full lines are the model calculations according to eq 2. **(b)** Influence of the activity coefficients on the Gibbs excess concentration, Γ_{21}, of propanone in the system toluene (1) + propanone (2) obtained by surface tension measurements: using eq 3 (full lines, Γ_{real}) and eq 4 (dashed lines, Γ_{ideal}). (A) T = 287.81 K; (B) T = 297.82 K; (C) T = 307.86 K; (D) T = 317.86 K.

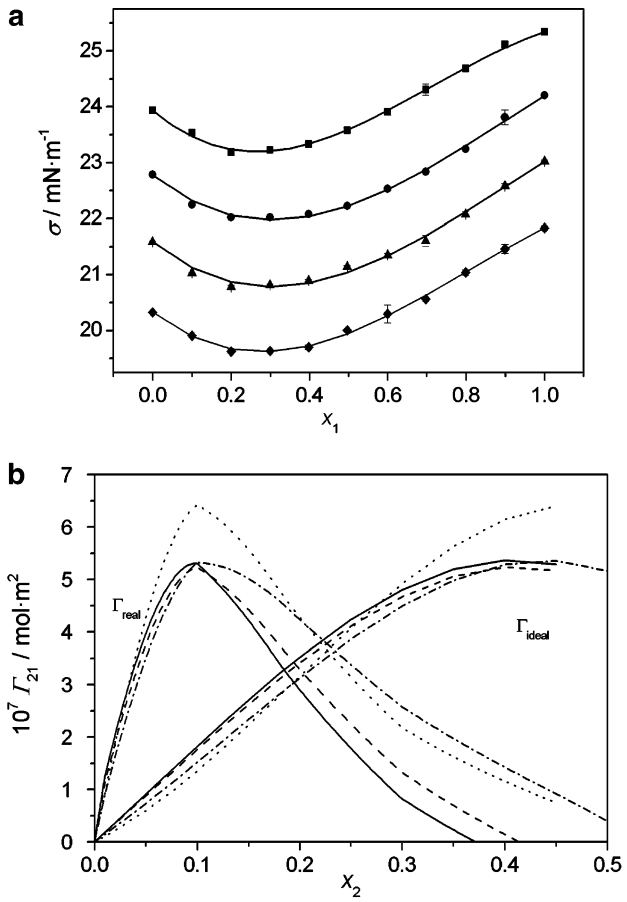

Figure 4. **(a)** Experimental surface tension, σ, of the binary mixtures of cyclohexane (1) + propanone (2) measured with the pendant drop apparatus: ■, T = 287.81 K; ●, T = 297.82 K; ▲, T = 307.86 K; ◆, T = 317.86 K. The full lines are the model calculations according to eq 2. **(b)** Influence of the activity coefficients on the Gibbs excess concentration, Γ_{21}, of propanone in the system cyclohexane (1) + propanone (2) obtained by surface tension measurements: using eq 3, Γ_{ideal}, and eq 4, Γ_{real}, at T = 287.81 K (dotted line), T = 297.81 K (solid line), T = 307.86 K (dashed line), and T = 317.86 K (dashed dotted line).

In Figure 2b the relative Gibbs excess concentrations Γ_{21} versus concentration are shown for the system cyclohexane (1) + heptane (2). For a given concentration x_2 at different temperatures, the gradient $(\partial\sigma/\partial x_2)_{T,p}$ is nearly constant. Therefore, the relative Gibbs excess concentration Γ_{21} will decrease with increasing temperature (A, B, C, and D). To show the effect of the thermodynamic activity coefficients, γ_2, over the simplified "ideal mixture" approach, the Γ_{21} values are calculated according to eq 3 (solid line) and eq 4 (dotted line). The thermodynamic activity coefficients, γ_2, were obtained from NRTL-parameters.[24] When we compare the "real" Γ_{21} with the "ideal" ones, we find almost no difference in the slopes. This indicates the marginal influence of activity coefficients in this nearly ideal system.

A different slope of surface tension versus concentration is found in the system propanone (1) + toluene (2) (Figure 3a). Contrary to the case of the mixtures containing cyclohexane + heptane, a positive deviation from linearity has been observed. Again, the parametrization gives a good representation of experimental data.

Figure 3b shows the relative Gibbs excess concentrations Γ_{21} against concentration range for this system. The differences from Γ_{real} to Γ_{ideal} of mixtures of toluene (1) + propanone (2) are slightly larger than those for the system cyclohexane + heptane.

Surface tension measurements of cyclohexane (1) + propanone (2) mixtures exhibit a strong negative deviation from ideality. The data together with their parametrization are shown in Figure 4a. At about 0.25 mol % of cyclohexane, we find a minimum in surface tension, which seems to be almost temperature independent. This minimum corresponds to a minimum in liquid densities (Table 4). At the lowest temperature, however, an inflection point might exist at very high concentration of cyclohexane. The density of pure cyclohexane is lower than that of propanone, whereas the surface tension of propanone is larger. A slight increase of surface tension up to the values of propanone at small cyclohexane ratios would be compensated by the density effect.

A striking influence of the activity coefficients on the relative Gibbs excess concentrations Γ_{21} is found in the system cyclohexane (1) + propanone (2). When we take the activity coefficients into account, the Gibbs excess concentration shows a distinct maximum at low propanone concentrations, which indicates a considerable enrichment of propanone within the interface. At higher concentrations of propanone, we will expect a depletion of propanone within the surface (Figure 4b). Experimental errors in the surface tension measurements strongly influence Γ_{21}, so that curves intersect each other and no clear temperature dependence can be found (Figures 3b and 4b). The enrich-

Table 8. Experimental Liquid Densities, $\rho^{I,II}$, and Density Differences, $\Delta\rho$, from 293.16 K to 357.96 K between the Two Liquid Phases of Mixtures of Heptane + *N*,*N*-Dimethylformamide, Heptane + *N*-Methyl-2-pyrrolidone, and Decane + *N*,*N*-Dimethylformamide Measured by Buoyancy Experiments

T	ρ^{I}	ρ^{II}	$\Delta\rho$	T	ρ^{I}	ρ^{II}	$\Delta\rho$
K	g·cm^{-3}	g·cm^{-3}	g·cm^{-3}	K	g·cm^{-3}	g·cm^{-3}	g·cm^{-3}
			Heptane + *N*,*N*-Dimethylformamide				
298.21	0.6893	0.9060	0.2166	341.46	0.7059	0.7771	0.0713
303.17	0.6863	0.8973	0.2109	341.46	0.7053	0.7771	0.0719
308.12	0.6844	0.8883	0.2039	341.85	0.7056	0.7802	0.0746
313.10	0.6831	0.8785	0.1954	341.95	0.7085	0.7784	0.0698
318.05	0.6799	0.8679	0.1880	342.05	0.7082	0.7767	0.0686
323.02	0.6820	0.8557	0.1737	342.16	0.7103	0.7749	0.0646
332.94	0.6857	0.8256	0.1399	342.16	0.7109	0.7755	0.0646
335.41	0.6884	0.8158	0.1274	342.25	0.7125	0.7735	0.0610
337.89	0.6932	0.8052	0.1120	342.25	0.7123	0.7735	0.0612
338.89	0.6956	0.7994	0.1037	342.35	0.7171	0.7672	0.0501
339.89	0.6995	0.7928	0.0933	342.40	0.7190	0.7659	0.0468
340.36	0.7005	0.7884	0.0880	342.45	0.7202	0.7644	0.0443
340.48	0.7023	0.7877	0.0855	342.51	0.7218	0.7617	0.0399
340.48	0.7008	0.7877	0.0870	342.56	0.7196	0.7586	0.0390
340.87	0.7043	0.7849	0.0806	342.60	0.7258	0.7558	0.0300
340.88	0.7023	0.7838	0.0815	342.64	0.7253	0.7506	0.0253
340.88	0.7030	0.7838	0.0808	342.64	0.7254	0.7506	0.0252
341.18	0.7044	0.7808	0.0764				
			Heptane + *N*-Methyl-2-pyrrolidone				
293.16	0.70523	0.9717	0.26647	324.25	0.7457	0.8544	0.1087
298.15	0.70783	0.9621	0.25427	325.25	0.7550	0.8420	0.0870
298.19	0.7070	0.9587	0.2517	325.35	0.7568	0.8397	0.0829
303.15	0.7095	0.9488	0.2393	325.45	0.7575	0.8389	0.0814
303.16	0.7059	0.9460	0.2401	325.46	0.7523	0.8448	0.0925
308.13	0.7080	0.9329	0.2249	325.45	0.7543	0.8428	0.0885
308.15	0.7112	0.93519	0.22400	325.55	0.7566	0.8398	0.0832
313.08	0.7143	0.9171	0.2028	325.65	0.7571	0.8392	0.0821
313.16	0.7146	0.9149	0.2003	326.31	0.7654	0.8279	0.0625
318.05	0.7203	0.8986	0.1783	326.40	0.7742	0.8154	0.0412
318.15	0.7227	0.8944	0.1717	326.40	0.765	0.8223	0.0573
322.49	0.7323	0.8753	0.1430	326.48	0.7679	0.8195	0.0609
323.26	0.7394	0.8634	0.1240	326.49	0.7675	0.8284	0.0516
			Decane + *N*,*N*-Dimethylformamide				
298.16	0.7315	0.9256	0.1941	348.15	0.7190	0.8362	0.1173
303.15	0.7283	0.9188	0.1905	350.66	0.7210	0.8274	0.1064
308.15	0.7260	0.9118	0.1858	350.66	0.7210	0.8280	0.1070
313.15	0.7238	0.9046	0.1808	353.15	0.7248	0.8177	0.0929
318.16	0.7217	0.8970	0.1752	354.15	0.7269	0.8134	0.0866
323.16	0.7194	0.8890	0.1697	355.15	0.7295	0.8078	0.0783
328.15	0.7180	0.8805	0.1625	356.16	0.7333	0.8015	0.0682
333.15	0.7163	0.8712	0.1549	357.16	0.7397	0.7926	0.0529
338.15	0.7162	0.8614	0.1452	357.65	0.7449	0.7856	0.0407
340.66	0.7166	0.8557	0.1391	357.75	0.7462	0.7841	0.0380
343.15	0.7170	0.8496	0.1326	357.85	0.7463	0.7840	0.0378
345.65	0.7177	0.8429	0.1252	357.96	0.7491	0.7809	0.0318
348.16	0.7190	0.8357	0.1167				

ment effects within the surface layer are experimentally very difficult to identify.[25−27] However, density functional theory and density gradient theory or molecular simulations are good theoretical methods or tools to predict such enrichment effects.[6,27]

Interfacial Tension. We applied the pendant drop method to perform measurements of interfacial tensions in systems with liquid−liquid phase separation. Here we can extend the measurements over a wide temperature range up to the critical solution point. Three systems of alkane + selective solvent (*N*,*N*-dimethylformamide, *N*-methyl-2-pyrrolidone) with upper critical solution points have been studied. Liquid densities and interfacial tensions of heptane + *N*,*N*-dimethylformamide, heptane + *N*-methyl-2-pyrrolidone, and decane + *N*,*N*-dimethylformamide were investigated from room temperature up to the critical solution temperature. Since the density difference between both liquid phases has a great influence on the resulting interfacial tension from the pendant drop image evaluation,

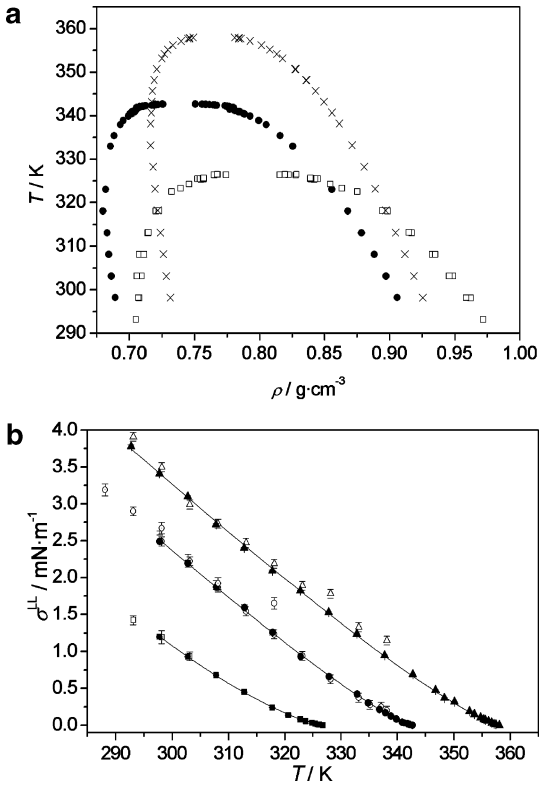

Figure 5. (a) Experimental liquid densities, ρ, from 290 K to 360 K measured with the buoyancy method: ●, heptane + *N*,*N*-dimethylformamide; □, heptane + *N*-methyl-2-pyrrolidone; ×, decane + *N*,*N*-dimethylformamide. **(b)** Experimental interfacial tension, σ, from 290 K to 360 K measured with the pendant drop apparatus: ●, heptane + *N*,*N*-dimethylformamide; ■, heptane + *N*-methyl-2-pyrrolidone; ▲, decane + *N*,*N*-dimethylformamide. Open symbols show drop volume measurements obtained from Wadewitz.[30] Solid lines are fitting results from eq 6 with the parameters ρ^{oLL} and σ^{o} and A_σ given in Table 11.

we applied bouyancy experiments as described above to measure the density in both phases. The density difference was calculated (Table 8).

These density measurements showed an accuracy of $\Delta\rho = \pm 0.0005$ g·cm^{-3}. Table 8 summarizes the corresponding liquid densities for the three mixtures at several temperatures.

Figure 5a presents our experimental results for the systems heptane + *N*,*N*-dimethylformamide, heptane + *N*-methyl-2-pyrrolidone, and decane + *N*,*N*-dimethylformamide. Since we extended our measurements to temperatures very close to the critical solution point, the density differences should be described by the following expression

$$\Delta\rho = \rho^{oLL}\left(1 - \frac{T}{T_c}\right)^{0.325}\left[1 + A_\rho\left(1 - \frac{T}{T_c}\right)^{0.5} + B_\rho\left(1 - \frac{T}{T_c}\right)^{1.0} + ...\right] \quad (5)$$

where, in addition to the classical term, Wegener expansion type parameters are included. This will improve the description in the near-critical region. In eq 5 we treat ρ^{oLL}, A_ρ, B_ρ, and the critical temperature T_c as free parameters. With the help of the Wegener expansion, the modeling of density differences from noncritical to near-critical regions was possible. In our model the Wegener exponent and the critical exponent $\beta = 0.325$ were fixed and as few as possible Wegener exponents were used.[29]

Table 9. Wegener Exponents, $\rho^{\circ LL}$, and Parameters, A_ρ, B_ρ, and T_c from Eq 5 To Describe the Liquid Densities of the Systems Heptane + *N*,*N*-Dimethylformamide, Heptane + *N*-Methyl-2-pyrrolidone, and Decane + *N*,*N*-Dimethylformamide

	$\rho^{\circ LL}$/g·cm^{-3}	A_ρ	B_ρ	T_c/K
heptane + *N*,*N*-dimethylformamide	0.4713 ± 0.007	−0.2873 ± 0.050	0	342.698 ± 0.016
heptane + *N*-methyl-2-pyrrolidone	0.4678 ± 0.034	1.958 ± 0.825	−4.369 ± 4.550	326.783 ± 0.077
decane + *N*,*N*-dimethylformamide	0.3895 ± 0.003	−0.2470 ± 0.022	0	358.083 ± 0.016

Table 10. Experimental Interfacial Tensions, σ^{LL}, of the Mixtures Heptane + *N*,*N*-Dimethylformamide, Heptane + *N*-Methyl-2-pyrrolidone, and Decane + *N*,*N*-Dimethylformamide Measured with the Pendant Drop Apparatus from 297.83 K to 357.45 K

heptane + *N*,*N*-dimethylformamide		heptane + *N*-methyl-2-pyrrolidone		decane + *N*,*N*-dimethylformamide	
T/K	σ^{LL}/mN·m^{-1}	*T*/K	σ^{LL}/mN·m^{-1}	*T*/K	σ^{LL}/mN·m^{-1}
297.83	2.49 ± 0.01	297.76	1.202 ± 0.008	292.78	3.780 ± 0.02
302.83	2.19 ± 0.05	302.78	0.930 ± 0.002	297.77	3.410 ± 0.02
307.85	1.87 ± 0.03	307.81	0.680 ± 0.004	302.79	3.100 ± 0.01
312.85	1.59 ± 0.01	312.84	0.450 ± 0.002	307.81	2.720 ± 0.01
317.86	1.26 ± 0.04	317.79	0.240 ± 0.002	312.79	2.400 ± 0.01
322.86	0.930 ± 0.01	320.65	0.137 ± 0.003	317.80	2.090 ± 0.01
327.88	0.660 ± 0.02	322.80	0.079 ± 0.002	322.78	1.820 ± 0.01
332.88	0.420 ± 0.02	323.75	0.055 ± 0.001	327.81	1.530 ± 0.01
334.87	0.302 ± 0.02	324.80	0.033 ± 0.004	332.81	1.240 ± 0.01
336.86	0.213 ± 0.01	325.43	0.019± 0.005	337.76	0.950 ± 0.005
337.88	0.169 ± 0.008	325.81	0.012 ± 0.002	342.78	0.690 ± 0.005
338.88	0.122 ± 0.002	326.10	0.009 ± 0.001	346.80	0.480 ± 0.004
339.87	0.086 ± 0.003			348.32	0.370 ± 0.004
340.87	0.042 ± 0.002			350.11	0.320 ± 0.002
341.25	0.032 ± 0.003			352.77	0.190 ± 0.002
341.88	0.020 ± 0.002			353.65	0.150 ± 0.004
342.18	0.011 ± 0.002			354.76	0.105 ± 0.003
				355.31	0.083 ± 0.003
				355.62	0.070 ± 0.002
				356.15	0.056 ± 0.003
				356.72	0.035 ± 0.003
				357.15	0.019 ± 0.003
				357.45	0.012 ± 0.002

Table 11. Parameters, $\sigma^{\circ LL}$ and A_σ, Describing the Interfacial Tension after Eq 6 for Heptane + *N*,*N*-Dimethylformamide, Heptane + *N*-Methyl-2-pyrrolidone, and Decane + *N*,*N*-Dimethylformamide

	$\sigma^{\circ LL}$/mN·m^{-1}	A_σ/mN·m^{-1}
heptane + *N*,*N*-dimethylformamide	39.086 ± 0.749	−0.467 ± 0.049
heptane + *N*-methyl-2-pyrrolidone	19.204 ± 0.548	1.099 ± 0.136
decane + *N*,*N*-dimethylformamide	38.381 ± 0.640	−0.392 ± 0.037

Table 9 gives the parameters obtained for the three systems studied. Only in the system heptane + *N*-methyl-2-pyrrolidone are two Wegener parameters necessary.

In Figure 5b experimentally determined interfacial tensions for the three systems (heptane + *N*,*N*-dimethylformamide, heptane + *N*-methyl-2-pyrrolidone, decane + *N*,*N*-dimethylformamide) are compared with results of other methods.[30] Using our pendant drop apparatus, the investigation of the critical region becomes possible. Other methods, for example, the ring method or drop volume method, are not able to measure interfacial tensions lower than 0.25 mN·m^{-1}.[30] Table 10 summarizes the experimental interfacial tensions of the three investigated systems together with their standard derivation. The experimental data can be represented by the following expression with Wegener expansion terms included.

$$\sigma = \sigma^{\circ LL}\left(1 - \frac{T}{T_c}\right)^{1.26}\left[1 + A_\sigma\left(1 - \frac{T}{T_c}\right)^{0.5} + ...\right] \qquad (6)$$

The critical temperature T_c is obtained from the density parametrization above, and the parameters $\sigma^{\circ LL}$ and A_σ are fitted to experimental data, given in Table 11.

Figure 5b shows the good quality of fitting to the experimental data of interfacial tensions in a wide temperature range starting from room temperature and extending up to the critical region.

Conclusions

Surface tensions of three liquid mixtures versus temperature were measured with a high precision pendant drop apparatus. Experimentally obtained surface tensions were correlated with a simple cubic polynomial in mole fraction. Gibbs excess concentrations, obtained from experimental surface tensions, showed enrichment effects for the system cyclohexane + propanone. The pendant drop apparatus is suitable for measuring interfacial tensions in systems with liquid−liquid phase separation. With density differences obtained by buoyancy experiments, the measurement of interfacial tension could be extended up to the critical region.

Literature Cited

(1) Wohlfarth, Ch.; Wohlfarth, B. Numerical Data and functional Relationships in Science and Technology. In *Surface Tension of pure Liquids and Binary Liquid Mixtures*; Lechner, M. D., Ed.; Landoldt-Börnstein New Series Group IV Physical Chemistry, Vol. 16; Springer: Heidelberg, 1997.

(2) Jasper, J. J. The Surface tension of pure liquid compounds. *J. Phys. Chem. Ref. Data* **1972**, *1* (4), 841−1009.

(3) Daubert, T. E.; Danner, R. P. *Physical and Thermodynamic Properties of Pure Chemicals*: *Data Compilation*; Hemisphere: New York, 1989.

(4) Poling, B. E.; Prausnitz, J. M.; O'Connell, J. P. *The Properties of Gases and Liquids*; MacGraw Hill: New York, 2001.

(5) Kahl, H.; Enders, S. Calculation of surface properties of pure fluids using density gradient theory and SAFT-EOS. *Fluid Phase Equilib.* **2000**, *172*, 27−42.

(6) Kahl, H.; Enders, S. Interfacial properties of binary mixtures. *Phys. Chem. Chem. Phys.* **2002**, *4*, 931−936.

(7) Wadewitz, T.; Winkelmann, J. Density functional theory: X-ray studies of pure fluid liquid/vapour interfaces. *Phys. Chem. Chem. Phys.* **1999**, *1*, 3335−3343.

(8) Winkelmann, J. The liquid−vapor interface of pure fluids and mixtures: application of computer simulation and density functional theory. *J. Phys. Condens. Matter* **2001**, *13*, 4739−4768.
(9) Rotenberg, Y.; Boruvka, L.; Neumann, A. W. Determination of surface tension and contact angle from the shapes of axisymmetric fluid interfaces. *J. Colloid Interface Sci.* **1983**, *93*, 169−183.
(10) Cheng, P.; Li, D.; Boruvka, L.; Rotenberg, Y.; Neumann, A. W. Automation of axisymmetric drop shape analysis for measurements of interfacial tensions and contact angles. *Colloids Surf.* **1990**, *43*, 151−167.
(11) Anastasiadis, S. H.; Chen, J. K.; Koberstein, J. T.; Siegel, A. F.; Sohn, J. E.; Emerson, J. A. The determination of interfacial tension by video image processing of pendant fluid drops. *J. Colloid Interface Sci.* **1987**, *119*, 55−66.
(12) Girault, H. H. J.; Schiffrin, D. J.; Smith, B. D. V. The measurement of interfacial tension of pendant drops using a video image profile digitizer. *J. Colloid Interface Sci.* **1984**, *101*, 257−266.
(13) Wiegand, G.; Franck, E. U. Interfacial tension between water and nonpolar fluids up to 473 K and 2800 bar. *Ber. Bunsen-Ges. Phys. Chem.* **1994**, *98*, 809−817.
(14) Dittmar, D.; Oei, S. B.; Eggers, R. Interfacial tension and density of ethanol in contact with carbon dioxide. *Chem. Eng. Technol.* **2002**, *25*, 23−27.
(15) Dittmar, D.; Eggers, R.; Kahl, H.; Enders, S. Measurement and modeling of the interfacial tension of triglyceride mixtures in contact with dense gases. *Chem. Eng. Sci.* **2002**, *57*, 355−363.
(16) Kreuser, H. Untersuchung von kritischen und nicht-kritischen Phasengrenzen in binären flüssigen Mischungen mit Mischungslücke. Ph.D. Thesis, University of Cologne, 1992.
(17) Mainzer, T. Diploma Work, University of Cologne, 1994.
(18) Wadewitz, T. Flüssige Grenzphasensysteme: Struktur, optische und Grenzflächeneigenschaften. Ph.D. Thesis, University of Halle Wittenberg, 1999.
(19) Kahl, H.; Wadewitz, T.; Winkelmann, J. Surface Tension of Pure Liquids and Binary Liquid Mixtures. *J. Chem. Eng. Data* **2003**, *48*, 580−586.
(20) Lahooti, S.; Del Rio, O. I.; Neumann, A. W.; Cheng, P. Axisymmetric drop shape analysis (ADSA). *Surfactant Sci. Ser.* **1996**, *63* (Applied Surface Thermodynamics), 441−507.
(21) Vargaftik, N. B. *Tables on the Thermophysical Properties of Liquids and Gases in Normal and Dissociated States*, 2nd ed.; 1975; 758 pp.
(22) Chaar, H.; Moldover, M. R.; Schmidt, J. W. Universal amplitude ratios and the interfacial tension near consolute points of binary liquid mixtures. *J. Chem. Phys.* **1986**, *85*, 418−427.
(23) Herrmann, L. Untersuchung von Struktur- und Grenzflächeneigenschaften binärer Systeme. Diploma Work, University of Halle, 1994.
(24) Paschke, A.; Bittrich, H. J. Modeling of the liquid/liquid equilibrium in the system heptan-toluene-*N*,*N*-dimethylformamide. *Chem. Tech.* (*Leipzig*) **1993**, *45*, 19−24.
(25) Dafay, R.; Prigogine, I.; Bellemanns, A.; Everett, D. H. *Surface Tension and Adsorption*; Wiley: New York, 1966.
(26) Adamson, A. W. *Physical Chemistry of Surfaces*; Wiley: New York, 1990.
(27) Schwuger, M. J. *Lehrbuch der Grenzflächenchemie*; Georg Thieme Verlag: Stuttgart, New York, 1996.
(28) Wadewitz, T.; Winkelmann, J. Density functional theory: structure and interfacial properties of binary mixtures. *Ber. Bunsen-Ges. Phys. Chem.* **1996**, *100*, 1825−1832.
(29) Greer, S. C.; Moldover, M. R. Thermodynamic anomalies at critical points of fluids. *Annu. Rev. Phys. Chem.* **1981**, *32*, 233−265.
(30) Wadewitz, T. Struktur und Grenzflächeneigenschaften binärer flüssiger Mischungen. Diploma Work, University of Halle, 1995.

Received for review March 28, 2003. Accepted September 4, 2003. The financial support of "Deutsche Forschungsgemeinschaft" (Wi 1081/6, 11) is gratefully acknowledged.

JE034062R